



permafrost
cci

**CCI+ PHASE 2 – NEW ECVS
PERMAFROST**

CCN4 OPTION 7

**ICEINSAR: INFERRED ACTIVE LAYER WATER/ICE
CONTENT AND FREEZE-THAW PROGRESSION FROM
ASSIMILATING INSAR IN PERMAFROST MODEL**

D2.2 ALGORITHM THEORETICAL BASIS DOCUMENT (ATBD)

VERSION 1.0

30 SEPTEMBER 2023

PREPARED BY

b·geos



GAMMA REMOTE SENSING

NORCE



UiO : University of Oslo

Document Status Sheet

Issue	Date	Details	Authors
0.1	18.07.2023	First template	LR
0.2	25.08.2023	First draft to co-authors	LR
0.3	24.09.2023	Second draft to co-authors	LR, LW
0.4	27.09.2023	Review from co-authors and correction	LR, LW, SW
1.0	30.09.2023	Review from all co-authors and correction to final version	LR, LW, SW, AB, TS

Author team

Line Rouyet and Lotte Wendt, NORCE

Sebastian Westermann, UiO

Annett Bartsch, B.GEOS

Tazio Strozzi, GAMMA

ESA Technical Officer

Frank Martin Seifert

EUROPEAN SPACE AGENCY CONTRACT REPORT

The work described in this report was done under ESA contract.
Responsibility for the contents resides in the authors or organizations that prepared it.

TABLE OF CONTENTS

Executive summary	4
1 Introduction	5
1.1 Purpose of the document	5
1.2 Structure of the document.....	5
1.3 Applicable Documents	5
1.4 Reference Documents.....	5
1.5 Bibliography	6
1.6 Acronyms.....	6
2 Scientific background.....	7
2.1 Current CCI products and limitations.....	7
2.2 Recent advances in transient permafrost modelling.....	7
2.3 InSAR for permafrost applications and link with physical modelling.....	8
3 Justification on the algorithm chosen	10
3.1 Summary of the user requirements	10
3.2 Contribution of Option 7 to fulfil the user requirements.....	10
4 Processing line.....	12
4.1 InSAR processing.....	12
4.1.1 <i>SAR images selection and interferogram generation</i>	12
4.1.2 <i>Small Baseline Subset (SBAS) processing</i>	13
4.1.3 <i>Results post-processing</i>	14
4.2 Subsurface modelling with CryoGrid community model.....	15
4.2.1 <i>Point-scale simulations in CryoGrid (prior to InSAR assimilation)</i>	16
4.2.2 <i>InSAR SD assimilation in CryoGrid point-scale simulations</i>	17
4.2.3 <i>Permafrost_cci regional products (baseline products)</i>	17
5 Required input data.....	18
5.1 InSAR processing	18
5.2 CryoGrid modelling.....	18
6 Output products	20
7 Practical considerations for implementation	21
8 References	22
8.1 Bibliography	22
8.2 Acronyms.....	24

EXECUTIVE SUMMARY

Within the European Space Agency (ESA), the Climate Change Initiative (CCI) is a global monitoring program which aims to provide long-term satellite-based products to serve the climate modelling and climate user community. The two main products associated to the ECV Permafrost are Ground Temperature (GT) and Active Layer Thickness (ALT). GT and ALT are documented by the Permafrost_cci project based on thermal remote sensing and physical modelling.

The Permafrost_cci models take advantage of additional datasets, such as snow cover and land cover, to estimate the heat transfer between the surface and the underground. However, several challenges remain due to spatially variable subsurface conditions, especially in relation to unknown amounts of water/ice in the active layer that modify the effective heat capacity and the thermal conductivity of the ground. In complex terrain with large spatial heterogeneities, coarse and partly inadequate land cover categorisation, the current results show discrepancies with in-situ measurements, which highlight the need to assimilate new data sources as model input. Although the ground stratigraphy is not directly observable from space, it impacts the dynamics of the ground surface. The seasonal thawing and refreezing induce cyclic subsidence and heave of the ground surface due to ice formation and melt in the active layer, and can therefore be used as indirect indicator of the ground conditions.

Synthetic Aperture Radar Interferometry (InSAR) based on Sentinel-1 images can be used to measure the amplitude and seasonal progression of these displacements. The movement amplitude is related to the amount of water/ice that is affected by a phase change, whilst the timing of the displacement patterns reflects the vertical progression of the thawing/freezing front. Considering the fine to medium spatial resolution of Sentinel-1 images, InSAR time series therefore have the potential to enhance the characterisation of subsurface hydrogeologic and thermal parameters and adapt the existing Permafrost_cci models to improve their performance at the local to regional scale. The *IceInSAR* pilot project (Option 7) will develop a prototype for permafrost model adjustment by assimilating Sentinel-1 InSAR surface displacement maps and time series into the model to constrain stratigraphy parameters. *IceInSAR* will provide pilot products, expected to be used for adjustment of the ECV processing chain of the baseline project in a next phase.

This Algorithm Theoretical Basis Document (ATBD) specifies the theoretical background of the algorithms and processing procedure used to develop the *IceInSAR* Option 7 products. The document provides a detailed description of the algorithm selected to generate the InSAR results and the strategy chosen to post-process the surface displacement (SD) products. The model to generate the ground temperature at a certain depth (GTD) and the active layer thickness (ALT) is described. A short reminder on the original Permafrost_cci processing line is provided before focusing on the specific components required by the Option 7. The required input data and the properties of the outputs are listed and practical considerations for the implementation of the processing lines are discussed.

1 INTRODUCTION

1.1 Purpose of the document

This document details the theoretical basis of the algorithms and processing lines selected to deliver the products of the Permafrost_cci *IceInSAR* Option 7. It has to be read as a complement to the PVASR [RD-5] and the ATBD from the baseline project [RD-6].

1.2 Structure of the document

Section 2 explains the scientific background of the *IceInSAR* Option 7 objectives and methods. Section 3 justifies the chosen algorithms and the processing procedure used to fulfil the Option 7 objectives, in respect with the user requirements [RD-1]. Section 4 describes the InSAR and CryoGrid processing lines used to generate the project outputs. Section 5 lists the required input data. Section 6 summarizes the expected outputs, in agreement with the PSD [RD-2]. Section 7 discusses practical considerations for the implementation of the Option 7 processing line.

A bibliography complementing the applicable and reference documents (Sections 1.3 and 1.4) is provided in Section 8.1. A list of acronyms is provided in Section 8.2. A glossary of the commonly accepted permafrost terminology can be found in [RD-15].

1.3 Applicable Documents

[AD-1] ESA. 2022. Climate Change Initiative Extension (CCI+) Phase 2 – New Essential Climate Variables – Statement of Work. ESA-EOP-SC-AMT-2021-27.

[AD-2] GCOS. 2022. The 2022 GCOS Implementation Plan. GCOS – 244 / GOOS – 272. Global Observing Climate System (GCOS). World Meteorological Organization (WMO).

[AD-3] GCOS. 2022. The 2022 GCOS ECVs Requirements. GCOS – 245. Global Climate Observing System (GCOS). World Meteorological Organization (WMO).

1.4 Reference Documents

[RD-1] Rouyet, L., Wendt, L., Westermann, S., Bartsch, A., Strozzi, T. 2023. ESA CCI+ Permafrost Phase 2. CCN4 Option 7. *IceInSAR*: Inferred Active Layer Water/Ice Content and Freeze-Thaw Progression From Assimilating InSAR in Permafrost Model. D.1.1 User Requirement Document (URD). Version 1.0. European Space Agency.

[RD-2] Rouyet, L., Wendt, L., Westermann, S., Bartsch, A., Strozzi, T. 2023. ESA CCI+ Permafrost Phase 2. CCN4 Option 7. *IceInSAR*: Inferred Active Layer Water/Ice Content and Freeze-Thaw Progression From Assimilating InSAR in Permafrost Model. D.1.2 Product Specification Document (PSD). Version 1.0. European Space Agency.

[RD-3] Bartsch, A., Matthes, H., Westermann, S., Heim, B., Pellet, C., Onaca, A., Strozzi, T., Kroisleitner, C., Strozzi, T. 2023. ESA CCI+ Permafrost Phase 2. D1.1 User Requirement Document (URD). Version 3.0. European Space Agency.

[RD-4] Bartsch, A., Westermann, S., Strozzi, T., Wiesmann, A., Kroisleitner, C., Wiczorek, M., Heim, B. 2023. ESA CCI+ Permafrost Phase 2. D1.2 Product Specification Document (PSD). Version 3.0. European Space Agency.

[RD-5] Bartsch, A., Westermann, S., Strozzi, T. 2023. ESA CCI+ Permafrost. D.2.1 Product Validation and Algorithm Selection Report (PVASR). Version 4.0. European Space Agency.

[RD-6] Westermann, S., Bartsch, A., Strozzi, T. 2023. ESA CCI+ Permafrost. D.2.2 Algorithm Theoretical Basis Document (ATBD). Version 4.0. European Space Agency.

[RD-7] Westermann, S., Bartsch, A., Heim, B., Strozzi, T. 2023. ESA CCI+ Permafrost. D.2.3 End-To-End ECV Uncertainty Budget (E3UB). Version 4.0. European Space Agency.

[RD-8] Westermann, S., Bartsch, A., Heim, B., Strozzi, T. 2023. ESA CCI+ Permafrost. D.2.4 Algorithm Development Plan (ADP). Version 4.0. European Space Agency.

[RD-9] Heim, B., Wiczorek, M., Pellet, C., Delaloye, R., Barboux, C., Westermann, S., Bartsch, A., Strozzi, T. 2023. ESA CCI+ Permafrost. D.2.5 Product Validation Plan (PVP). Version 4.0. European Space Agency.

[RD-10] Bartsch, A., Westermann, S., Strozzi, T. 2023. ESA CCI+ Permafrost. D.2.1 Product Validation and Algorithm Report (PVASR). Version 4.0. European Space Agency.

[RD-11] Heim, B., Lisovski, S., Wiczorek, M., Pellet, C., Delaloye, R., Bartsch, A., Jakober, D., Pointer, G., Strozzi, T. 2021. ESA CCI+ Permafrost. D.4.1 Product validation and intercomparison report (PVIR). Version 3.0.

[RD-12] Obu, J. Westermann, S., Strozzi, T., Bartsch, A. 2021. ESA CCI+ Permafrost. D.4.2 Climate Research Data Package Version 2 (CRDPv2).

[RD-13] Duchossois G., P. Strobl, V. Toumazou, S. Antunes, A. Bartsch, T. Diehl, F. Dinessen, P. Eriksson, G. Garric, M-N. Houssais, M. Jindrova, J. Muñoz-Sabater, T. Nagler, O. Nordbeck. 2018. User Requirements for a Copernicus Polar Mission - Phase 1 Report, EUR 29144 EN, Publications Office of the European Union, Luxembourg, 2018, ISBN 978-92-79-80961-3, <https://doi.org/10.2760/22832>, JRC111067.

[RD-14] Bartsch, A., G. Hugelius, Strozzi, T. 2021. ESA CCI+ Permafrost CCN3 Option 6: improved soil description through a landcover map dedicated for the Arctic. User Requirements Document, v1.0.

[RD-15] National Research Council. 2014. Opportunities to Use Remote Sensing in Understanding Permafrost and Related Ecological Characteristics: Report of a Workshop. Washington, DC: The National Academies Press. <https://doi.org/10.17226/18711>.

[RD-16] van Everdingen, Robert, Ed. 1998 revised May 2005. Multi-language glossary of permafrost and related ground-ice terms. Boulder, CO: National Snow and Ice Data Center/World Data Center for Glaciology. (<http://nsidc.org/fgdc/glossary/>; accessed 23.09.2009).

1.5 Bibliography

A complete bibliographic list that supports arguments or statements made within the current document is provided in Section 8.1.

1.6 Acronyms

A list of acronyms is provided in Section 8.2.

2 SCIENTIFIC BACKGROUND

2.1 Current CCI products and limitations

In the ESA GlobPermafrost project, a simple equilibrium permafrost model has been employed to infer ground temperatures and permafrost extent (Obu et al., 2019) based on thawing and freezing degree days derived from remotely sensed data, in particular Land Surface Temperature (LST). To account for the transient response of the ground thermal regime to a changing climate forcing, the Permafrost_cci project has developed a transient model based on the CryoGrid family of ground thermal models (Westermann et al., 2023).

CryoGrid uses a wide variety of forcing datasets, numerically solving the heat conduction equation including the phase change of water/ice in soil pores. The feasibility and maturity of the CryoGrid transient permafrost model in conjunction with EO-data over large spatial domains has been demonstrated in a pilot study in Northern Siberia (Westermann et al., 2016; 2017). Later on, the model has been applied at the global scale to generate the Permafrost_cci Phase 1 products [RD-12] (Obu et al., 2021a; 2021b; 2021c). EO-datasets are employed to determine the upper boundary condition of the differential equation, while its coefficients (e.g. heat capacity and thermal conductivity) are selected according to landcover information. However, several challenges remain due to spatially variable subsurface conditions, especially in relation to unknown amounts of water/ice in the active layer that modify the effective heat capacity and the thermal conductivity of the ground. In complex terrain with large spatial heterogeneities and coarse land cover categorisation, the current results show discrepancies with in-situ measurements [RD-11], which highlight the value of assimilating new data sources in the model. In the framework of the *IceInSAR* Option 7, we study how InSAR surface displacement (SD) measurements can be used as new data input.

2.2 Recent advances in transient permafrost modelling

Continued model development with a community of permafrost researchers recently led to the establishment of a CryoGrid community model (Westermann et al., 2023), which comprises the functionalities of all CryoGrid models in a modular framework. In CCI+ Phase 2 iteration 1, the Permafrost_cci model has been integrated as a new module in the CryoGrid community model, making it accessible to a wider user community [RD-6]. The community model is supplemented by new functionalities for generating model ensembles and ingesting various spatially distributed datasets. This development makes it possible to take advantage of the recent advances made by the community and to set up the adjusted Option 7 model within the CryoGrid community model.

Due to the modular design of the CryoGrid community model, different observation operators and subsurface models of varying complexity can be combined within the data assimilation procedure (Westermann et al., 2023). Various subsurface models are available in CryoGrid, in particular models in which the water/ice content is static against models which compute a full water balance, allowing for inflow from the sides or downward drainage. From these, the surface heave can be inferred by using the density difference between ice and water. Recent work extended the capabilities of CryoGrid to represent soil mechanical processes to simulate ice segregation and thaw consolidation (Aga et al., 2023). This new module produces much larger heave signals especially for organic soils, which may be in better agreement with observations than the “traditional” models.

To assimilate InSAR SD products, data assimilation methods are available in CryoGrid. In particular, iterative data assimilation techniques hold significant promise for complex models with many parameters that need to be jointly constrained. The data assimilation starts with more uncertain model properties, which are narrowed down in a first assimilation step by comparing the results to observations to generate a second ensemble with a narrower parameter range. The iterative procedure continues until the parameter set is optimised. Iterative data assimilation methods allow for working with fewer ensemble members and could also reduce the overall computational cost of the processing chain (Aalstad et al., 2018).

2.3 InSAR for permafrost applications and link with physical modelling

The ground stratigraphy and the ground thermal regime impact the dynamics of the ground surface. The seasonal thawing and refreezing induce cyclic subsidence and heave of the ground surface due to ice formation and melt in the active layer. In permafrost lowlands, the movement amplitude is related to the amount of water/ice that is affected by a phase change, while the timing of the displacement patterns reflects the vertical progression of the thawing/freezing front. These displacement patterns can be measured by comparing satellite images taken at different times. The use of spaceborne imaging Synthetic Aperture Radar (SAR) is especially suitable for remote sensing measurements in cold climate regions due its insensitivity to light and meteorological conditions. Using the phase component of the SAR images processed with SAR Interferometry (InSAR) algorithms, ground surface movement can be measured at centimetre to millimetre accuracy.

The launch of Sentinel-1 satellites has pushed forward the use of InSAR for permafrost applications and shows the value of extensive spatial coverage, weekly temporal resolution and open access imagery to map and monitor ground movement in cold climate regions. Sentinel-1 InSAR subsidence maps have been generated to document the spatial variability of the ground ice content and identify ice-rich areas (Bartsch et al., 2019; Rouyet et al., 2019; Wang et al., 2020; Zwieback et al., 2021). The movement amplitude in permafrost environments is highly related to the frost-susceptibility of the ground material, i.e. the ability for water to turn into ice lenses and lift up the ground surface during the freezing period. As frost-susceptibility depends on the material grain size, there is a relationship between the seasonal movement amplitude and the landcover type (Bartsch et al., 2019) or the geomorphological units (Rouyet et al., 2019) (**Figure 1A**), which can be used to infer geocryological conditions. Several studies have shown that Sentinel-1 InSAR time series can document fine temporal variability of subsidence and heave patterns, able to reflect the seasonal progression of thawing and freezing front in the active layer (Strozzi et al., 2018; Zhang et al., 2019; Reinosch et al., 2020; Rouyet et al., 2021) (**Figure 1B**). Seasonal time series can also be used to identify late-summer secondary subsidence patterns highlighting degradation of ice-rich layers at the top of the permafrost (Zwieback & Meyer, 2021).

The fine to medium resolution of Sentinel-1 InSAR maps and time series have the potential to enhance the characterisation of subsurface hydrogeologic and thermal parameters, in combination with physical modelling. Several studies have constrained the InSAR deformation algorithm based on physical permafrost models (Zhao et al., 2016; Wang et al., 2017; Zhang et al., 2020). Others have combined InSAR with simple physical models to estimate ALT or interpret the temporal dynamics of the ground (Liu et al., 2012; Schaefer et al., 2015; Wang et al., 2018; Rouyet et al., 2021). In the *IceInSAR* Option 7, we work towards assimilating InSAR surface displacement (SD) products into CryoGrid to constrain

the parametrization of the ground stratigraphy and potentially improve the performance of the model in complex terrain.

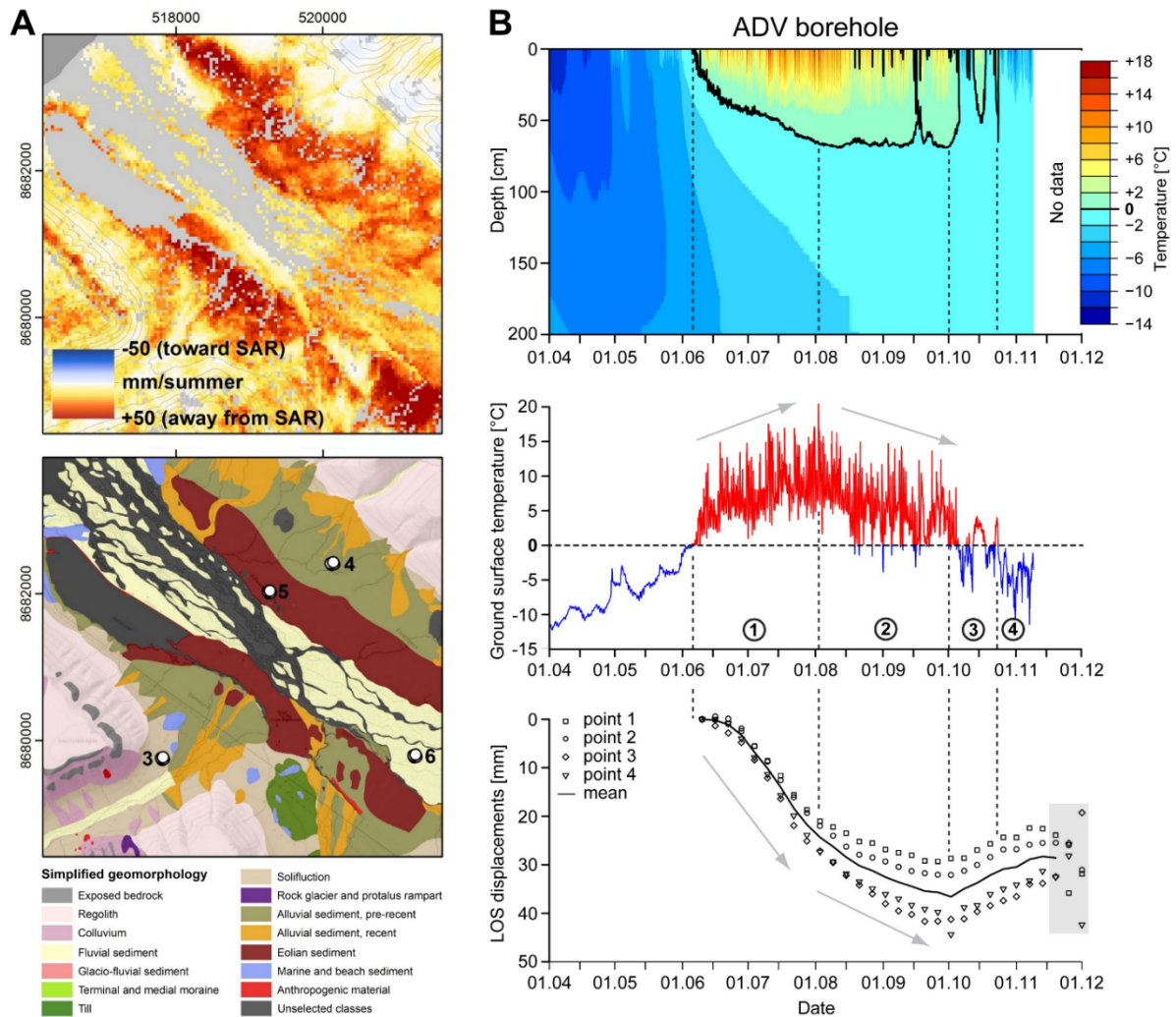


Figure 1: Examples of InSAR subsidence maps and seasonal thaw subsidence and frost heave time series that have the potential to be exploited for constraining the CryoGrid permafrost model. **A)** Comparison between thaw subsidence and geomorphological units in the bottom of Svalbard valley. **B)** Comparison between the in-situ temperature and subsidence/heave InSAR time series at the location of a borehole. Modified from Rouyet et al. (2019).

3 JUSTIFICATION ON THE ALGORITHM CHOSEN

3.1 Summary of the user requirements

The users demand a combination of high spatial and temporal resolution (URq_09, URq_12, URq_13, URq_18). The current Permafrost_cci products fulfil the threshold requirements of the Permafrost_cci users (1-km annual products) [RD-1]. However, several reference documents highlight the demand for higher spatial resolutions, especially valuable in areas where complex topography and heterogenous ground conditions may lead to poor model performance.

A high data quality and product accuracy is also required (URq_4, URq_9, URq_12, URq_13, URq_19). On average, the product accuracy of Permafrost_cci CRDPv2 fulfils the threshold requirements of the Permafrost_cci users (RMSE < 2.5 °C for GT and < 25 cm for ALT) [RD-1]. However, significant spatial heterogeneities and systematic biases in specific regions have been identified.

The users highlighted the value of enhanced ground stratigraphy products and the representation of the subgrid variability (URq_11, URq_12, URq_13, URq_21, URq_22) [RD-1]. The current model takes advantage of additional datasets, such as land cover, to estimate the heat transfer between surface and subsurface. The subgrid variability is documented based on the median and standard deviation of the model ensemble. However, several challenges remain due to spatially variable subsurface conditions, especially in relation with the unknown amounts of water/ice in the active layer. The water/ice content modifies the effective heat capacity and the thermal conductivity of the ground. In complex terrain with large spatial heterogeneities and coarse land cover categorisation, the current results show discrepancies with in-situ measurements, which highlights the need to assimilate new data sources as model input.

Finally, the potential of integrating surface displacement (SD) as new permafrost product is also highlighted in reference documents (URq_3, URq_20) [RD-1]. In addition to their assimilation into the Permafrost_cci model, the InSAR products from Option 7 can also have a standalone value, for both scientific and operation applications in Svalbard (auxiliary data for geomorphological mapping and permafrost model, concrete use for geohazard management, etc.).

3.2 Contribution of Option 7 to fulfil the user requirements

Downscaling the model results can become possible for targeted regions, by including complementary high-resolution input products, such as SD maps based on InSAR (initial resolution: 20x5 m for Sentinel-1 Interferometric Wide Swath images; final resolution after multi-looking: 40–100 m). Similarly, at the regional scale, the temporal resolution can realistically be increased to the target requirement (monthly), based on Land Surface Temperature diurnal data and InSAR-based thaw subsidence and frost heave time series with a 6–12 days temporal resolution. It should however be noted that the InSAR information will be spatially and temporally discontinuous. Areas affected by typical SAR geometrical limitations (shadow/layover) and interferometric coherence loss due to wet/snow-covered surfaces or fast displacements ($> \frac{1}{2}$ the wavelength during the time interval of the interferograms, i.e. about 2.8 cm in 6–12 days) will remain undocumented. Due to coherence loss during the winter, the InSAR time series will document the displacement progression during the snow-free seasons only (typically May–June to October–November in Svalbard).

Detailed analyses at the regional scale may contribute to further understand discrepancies between the model and in-situ validation data. Comparing the products from the initial model with the SD-

constrained model will allow to evaluate the potential of improving the model performance based on new data inputs. The high resolution of the InSAR data will also contribute to the representation of the natural subgrid variability, that will contribute to assess if the discrepancies between the model and the validation data are caused by biases or rather related to the natural spatial variability of permafrost parameters within the resolution cell.

The integration of InSAR data indirectly documenting the active layer ice content, the sediment type and ground freeze/thaw timing will be used to constrain specific ground stratigraphy parameters in the model, at a spatial resolution much higher than the global products. The downscaled results will provide a representation of the subgrid variability that will be compared with the median and standard deviation of the model ensemble for the 1-km grid. By comparing InSAR-based SD with acquired in-situ data, Option 7 will also show how the SD product may contribute to document the sediment type and ice/water content and thus complement the generation of new ground stratigraphy products.

The User Requirements of the Copernicus Polar Mission [RD-13] recognizes surface displacement (SD) as a key parameter for monitoring permafrost regions. The required spatial resolution of such products (goal: 1 m, threshold: 5 m) is higher than the possible resolution based on Sentinel-1 images, but can be fulfilled by satellites with higher spatial resolutions (e.g. TerraSAR-X, Radarsat-2). The required temporal resolution (goal: 14 days) can be met during the snow-free seasons (6–12 days InSAR time series). For the purpose of CryoGrid, threshold and target requirements for spatial resolution (100–300 m and 20 m) can however be met [RD-14]. The potential of using remotely sensed displacement maps to infer the active layer thickness or the ice/water content is widely recognized [RD-15] and may complement current products. Although the use of InSAR surface displacements in permafrost regions is still at a research stage (Strozzi et al., 2018; Bartsch et al., 2019; 2023; Rouyet et al., 2019; 2021; Zwieback & Meyer, 2021), the development of strategies for generating systematic products at the large scale are quickly advancing. The *IceInSAR* Option7 may contribute to design the procedure for delivering operational SD products in a future phase.

4 PROCESSING LINE

4.1 InSAR processing

The Option 7 SD products are processed with Synthetic Aperture Radar (SAR) Interferometry (InSAR) methods based on Sentinel-1 images. The Sentinel-1 satellites have active SAR sensors on board, which operate in the microwave domain (C-band with wavelength 5.6 cm). Image pairs (interferograms) are formed using the phase information recorded by the SAR sensor. By calculating the phase differences between two images taken from different acquisition times, we can measure how the ground surface has moved during the considered time interval.

The phase signal is cyclic, and each cycle represents half the wavelength as the radar signal travels to the ground and back to the sensor. The signal is therefore ambiguous and only displacements less than half the wavelength (e.g. ~ 2.8 cm for Sentinel-1) can be resolved for one interferogram. Aliasing can already occur when the displacement rate exceeds a quarter of the wavelength during the considered time interval (i.e. over 2.3 mm/day using 6-days Sentinel-1 interferograms). The detected displacements are spatially relative to a chosen reference point chosen in an area assumed to be stable and temporally relative to the first image acquisition of a time series.

InSAR measurements are one-dimensional. They correspond to the projection of the real ground surface displacements along the radar line-of-sight (LOS). The Sentinel-1 satellites follow a sun-synchronous polar orbit, and observes at an oblique incidence angle towards East (ascending passes) or West (descending passes). The results from one geometry can be projected based on the expected movement orientation (i.e. vertical with focusing on flat terrain affected by heave and subsidence).

InSAR results can be affected by various error sources, which require several steps of SAR image selection, interferogram filtering, quality check and selection, advanced time series generation and post-processing. The processing is performed with the NORCE in-house GSAR software (Larsen et al., 2005). The steps described in the following sections are performed for the three study areas (Adventdalen ADV, Ny-Ålesund NYA and Kapp Linné KL [RD-2]).

4.1.1 SAR images selection and interferogram generation

All available Sentinel-1 Interferometric Wide (IW) swath mode Single Look Complex (SLC) images between May and December 2016–2022 are downloaded. Available TerraSAR-X, PAZ, Radarsat-2 and ALOS-2 data may also be used to evaluate the effect of the spatial resolution and cross-validate results using different radar frequencies (Wang et al, 2020). We apply an InSAR technique employing complex spatial averaging (multi-looking) to improve the signal stability and dampen the influence of unrepresentative scattering effects within resolution cells (Berardino et al., 2002). For Sentinel-1 IW images, an 8x2 multi-looking factor (8 looks in range, 2 looks in azimuth) is applied, leading to a spatial resolution of approximately 40 m. Other multi-looking factors may be tested and compared. The noise-level is reduced in all interferograms by applying a spatially adaptive coherence-dependent Goldstein filter (Goldstein & Werner, 1998; Baran et al., 2003).

In permafrost environments, the spatio-temporal variability of the snow cover is the main challenge that can induce spatially and temporally discontinuous coverage of exploitable interferometric signals. The interferograms are generated within the main snow-free seasons, aiming for a fully connected network of image pairs (i.e. continuous series within each season). We focus on 2017–2021 seasons to have a 6-

days repeat-pass, but will also test the procedure for 2016, 2022 and 2023 (12-days repeat-pass). The interferogram selection is semi-automated. A first selection is performed using coherence statistics, a measure of the interferometric signal quality (Bamler & Hartl, 1998). The pre-selected set is then manually checked to discard interferograms with obvious localised decorrelation in areas affected by fast-moving, moist or snow-covered ground. The observation window is maximised for each season, starting from the first and ending with last snow-free images based on coherence values and available meteorological data. The time interval (temporal baseline) used to generate the image pairs depends on the coherence and the expected variability of the movement rate during the observation window. It practically means that only short interferograms (typically 6–18 days) are used at the start and the end of the season (due to rapid subsidence or heave, highly moist ground and minor snowfall). Interferograms with longer time intervals (up to 48 days) can often be used at the end of the thawing period (approximately between end of July and end of September).

Areas affected by geometric effects, such as layover, are masked out. The topographic component is removed using an external Digital Elevation Model (DEM) (20 m resolution in Svalbard; NPI, 2014). Pixels affected by low signal stability due to snow (e.g. perennial patches), water (e.g. lakes, rivers) or dense vegetation (e.g. forested areas) in most of the pairs were removed by applying a coherence-based filter (above 0.45-0.5 in at least 50% of the interferograms). If snow or surface water at one specific location is affecting too many interferograms in the stack (e.g. long-lasting snow patches, flooded area), the pixel is discarded.

The conversion from cyclic to continuous phase differences, so called unwrapping, is performed using the SNAPHU algorithm (Chen & Zebker, 2002). InSAR is a spatially relative technique, meaning that it must be calibrated to a reference location. Different reference points are tested and a common reference for all datasets is chosen in an area assumed to be stable.

The results of this first processing steps are the final sets of quality checked wrapped and unwrapped interferograms for all 2017–2021 snow-free seasons. To minimise the processing steps required for product generation before assimilation in the model, we will test the feasibility of using single interferograms as model inputs.

4.1.2 Small Baseline Subset (SBAS) processing

Single interferograms are expected to have a low signal-to-noise ratio due to the impact of unwanted phase components, such as the Atmospheric Phase Screen (APS) (Hanssen, 2001). We therefore process time series with the multi-temporal Small Baseline Subset (SBAS) algorithm (Berardino et al., 2002), which uses the redundancy of time-overlapping interferograms to mitigate the atmospheric component and improve the measurement accuracy. The phase inversion is performed using a L1-norm-based cost function, which is more robust than L2-norm with respect to unwrapping errors (Lauknes et al., 2010). For the atmospheric filtering, we used a spatial filter of 500 m and a temporal filter of 18 days. The initial SBAS results correspond to the line-of-sight (LOS) ground surface displacement at each documented pixel and for each time step of the series, expressed in mm.

Each snow-free season is processed separately. We do not connect images between the different summer seasons, as fast movement can occur in the winter periods and long interferograms may therefore lead to phase aliasing. As a result, each seasonal time series begins at 0 mm, even though there could potentially be some long-term subsidence over the years. For the similar observation periods and

acquisition times, coherence time series will be provided and expressed as values between 0 (low signal stability) and 1 (high signal stability). As an estimate of the phase standard deviation, coherence provides a measure of uncertainty (Bamler & Hartl, 1998) that can be used to weight the measurements in the CryoGrid model (see Option 7 E3UB).

4.1.3 *Results post-processing*

Several post-processing steps are applied on the initial SBAS results to filter out irrelevant pixels and focus on unambiguous time series. A secondary coherence thresholding (higher value) may be applied at the post-processing stage. Glacial areas are discarded using an external mask of glacier extents (König et al., 2013; Lith et al., 2021). Time series likely to be affected by phase ambiguities (phase changer larger than a quarter wavelength, i.e. 14 mm, between successive acquisition dates) are discarded. Sloping terrain (> 5 degrees) is discarded to focus on flat terrain assumed to be dominated by vertical displacements (i.e. strandflats, sediment-infilled valley bottoms, mountain plateaus) (Rouyet et al., 2021). Initial line-of-sight (LOS) SD are projected vertically. The results are geocoded using the available 20 m DEM (NPI, 2014). All final products have a spatial resolution corresponding to the chosen multi-looking factors (40 m when using an 8x2 multi-looking based Sentinel-1 IW data).

Based on the 6/12-days displacement times series, the transition between thaw subsidence and frost heave can be detected and the value of the maximal subsidence identified for each series (Rouyet et al., 2021). **The seasonal SD time series (SSD product**, as described in the PSD [RD-2]) will include the maximum subsidence value, the Day of Year (DOY) of the maximum subsidence and the vertical displacement and coherence time series for each documented pixel in flat terrain. The seasonal subsidence maps can be used to infer the seasonal active layer water/ice content.

The results can be mapped to document the spatio-temporal variability of the active layer water/ice content for each season. **Multi-seasonal SD maps (MSD product**, according to the properties described in the PSD [RD-2]) can be generated following two approaches:

- **Mean velocity maps** processed using a simple weighted averaging method, so-called stacking (Sandwell & Price, 1998). We include interferograms from the thawing periods only and average the velocity from all seasons, leading to one product for each SAR geometry (ascending and descending mean velocity maps). The results are expressed in mm/summer. The summer is defined here as the averaged thawing period based on the available interferograms and auxiliary meteorological data (NCCS, 2023). It typically lasts between 3 and 4 months in the study areas.
- **Multi-seasonal average of the maximal subsidence** extracted from each SBAS time series. The extracted maximal subsidence values for each season can be averaged to provide a multi-seasonal product for each SAR geometry. The results are expressed in mm.

Both maps should overall highlight the same spatial patterns but may display fine-scale discrepancies considering that the stacking method linearly averages the subsiding rates during the thawing periods, whilst the multi-season maximum subsidence map accounts for the accumulated final displacement without considering potentially variable subsidence rates during the thawing periods. Both maps will be compared, and their potential differences discussed.

The SSD and MSD products will be used as model inputs (see Section 4.2) to evaluate how they contribute to improve the model performance by constraining the parametrization of the ground

stratigraphy based on the subsidence patterns during the thawing season and the distribution of the movement amplitude. Subproducts such as InSAR-based geocryological maps clustering the InSAR information in a few ground movement categories may also be tested for assimilation in the model (see Option 7 ADP).

4.2 Subsurface modelling with CryoGrid community model

Simulations of subsurface temperatures is based on the CryoGrid community model (Westermann et al., 2023), which comprises both the functionality of the Permafrost_cci model used for the baseline project, as well as more sophisticated, but computationally demanding process models. Some modules from the CryoGrid community models process models can account for the complex water cycle of the permafrost and are therefore well suited for simulating the variability of active layer water/ice content (e.g. Westermann et al., 2016). The theoretical basis is detailed in Westermann et al. (2023) and the ATBD of the baseline project [RD-6]. **Figure 2** shows a schematic representation of the CryoGrid Permafrost_cci model used for the baseline project, summarising the main input data and parameters that need to be set to provide depth- and time-resolved fields of ground temperatures are derived. For this scheme, suitable land surface temperatures (LST) products from satellites are only available at 1-km scale, thus limiting the spatial resolution. In *IceInSAR* Option 7, we will therefore explore other subsurface model types (which all are available in the CryoGrid community model, see below) which are driven by near-surface meteorological variables and can thus be run at the higher spatial resolutions of InSAR SD products.

The assimilation of InSAR SD products will allow for constraining the subsurface properties shown on the left of the sketch. A prototype for ensemble-based data assimilation with the particle filter is already implemented in the CryoGrid community model and will be explored and if necessary modified/extended in the *IceInSAR* Option 7.

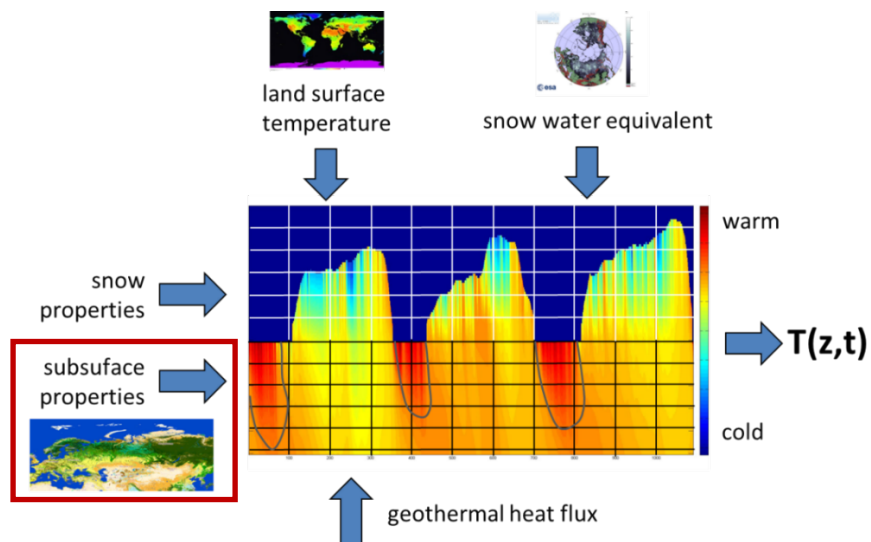


Figure 2: Schematic representation of the CryoGrid Permafrost_cci model scheme, showing the input data land surface temperature and snow water equivalent for which time series are required. Snow properties are computed by the model scheme, while subsurface properties are assigned based on the ESA CCI landcover product. At the lower boundary of the model domain, a (constant) geothermal heat flux is prescribed. CryoGrid CCI delivers depth- and time-resolved fields of ground temperatures, from which annual averages at different depths, from which annual active layer thickness are derived (from thaw progression, grey line) [RD-6]. In the Option 7, InSAR SD will be used to refine subsurface parametrization (red rectangle).

In the following sections, we only summarize elements that have specific implications for the Option 7 processing line. We focus here on describing the modifications required to assimilate InSAR-based SD products in CryoGrid.

In the Option 7, the ground temperature at a certain depth (maximum 5 m) (GTD) and the active layer thickness (ALT) will be modelled at two spatial scales:

- **Proof-of-concept products at the local scale:** One-dimensional point-scale simulations will be performed at selected locations with available near-surface meteorological data. The results will be directly comparable with GTD and ALT from permafrost monitoring in boreholes. The model will be run before and after assimilation of the InSAR SD products to compare the performance. The local products will have a daily resolution.
- **Experimental products at the regional scale:** The model will be driven by downscaled ERA-5 reanalysis data in the selected study areas. The model will be run before and after the assimilation of InSAR SD products. While the baseline Permafrost_cci product has a 1-km resolution, the results after the SD assimilations will be at the higher resolution of the InSAR SD products (40–100 m). The regional products will have a one-year temporal resolution, corresponding to the average mean annual ground temperature and the maximum depth of seasonal thaw (active layer thickness).

Considering the period for which we will process the SD products (see Section 4.1.1), we will essentially focus on the same years (2017–2021 with 6d repeat pass; 2016, 2022 and 2023 with 12d repeat pass) for testing the assimilation procedure and generating GTD and ALT. The model spin-up largely follows the accelerated spin-up procedure described in the Section 3.1.4 of Westermann et al. (2023).

4.2.1 *Point-scale simulations in CryoGrid (prior to InSAR assimilation)*

Different ground models are already available in CryoGrid, in particular models in which the water/ice content is static against models which compute a full water balance, allowing for inflow from the sides or downward drainage. We will test and, if necessary, modify these ground models. To apply data assimilation, the creation of synthetic observations from the model states of the ensemble is needed, which requires observation operators computing subsidence and heave signals.

We will compute the subsidence/heave patterns from the change in active layer water/ice content and the density difference of water and ice. We will develop a parametrisation for unsaturated soils, which are expected to heave when the water content is high, while the ice expands in the pore space for dry soil conditions. If needed, we will explore a new module for segregated ice formation within the CryoGrid community model (Aga et al., 2023) which is able to produce larger heave signals especially for organic soils, which may improve the agreement with observations. Due to the modular design of the CryoGrid community model, we can flexibly combine different observation operators and subsurface models of different complexity within the data assimilation procedure.

The data assimilation procedure starts with the generation of a model ensemble that simulates the initial uncertainty (prior to assimilation of InSAR data) of the subsurface properties and other factors used as model inputs. We will investigate how the choice of this initial state of the model ensemble and its uncertainty impacts the performance of the data assimilation.

4.2.2 *InSAR SD assimilation in CryoGrid point-scale simulations*

The particle filter implemented in CryoGrid provides a suitable starting point to test assimilation of InSAR time series. We will in particular evaluate the optimal size of the model ensemble needed to avoid problems with degeneracy, while at the same time being feasible to run on the available high-performance computing systems. Furthermore, we will test if iterative data assimilation methods are required. These allow to start with more uncertain model properties, which are narrowed down in a first assimilation step by comparing the results to the InSAR observations to generate a second ensemble with a narrower parameter range. The iterative procedure continues until the parameter set is optimised. Iterative data assimilation methods allow for working with fewer ensemble members and could also reduce the overall computational cost of the processing chain (Aalstad et al., 2018).

4.2.3 *Permafrost_cci regional products (baseline products)*

To provide a state-of-the-art reference for the InSAR SD assimilation, the baseline Permafrost_cci GTD and ALT products will be extracted within the three study areas (Adventdalen, Ny-Ålesund and Kapp Linné [RD-2]). The spatial resolution is limited to 1 km, which is the spatial resolution of the remotely sensed LST, but ensemble-based modelling of subpixel variability of subsurface properties is applied. With this, different ensemble members can represent different ground stratigraphies and snow depths found within the 1 km pixels, which is required for computation of permafrost and talik fractions within a pixel. For each 1-km pixel, the baseline product provides time series of surface temperature, snowfall and snowmelt which can be compared to InSAR SD products.

4.2.4 *InSAR SD assimilation in experimental regional products*

Considering the specific objective of assimilating InSAR products within the model, the regional GTD and ALT products of the *IceInSAR* Option 7 will be downscaled based on the higher resolution InSAR-based SD products. The variability of the results within a 1 km grid of the initial Permafrost_cci products will be compared with the results from the representation of subpixel variability based on ensemble-based modelling (Section 4.2.3). Model applications at the regional scale require the generation of a suitable model forcing by downscaling ERA-5 reanalysis for the study areas, using the TopoScale downscaling routine (Fiddes & Gruber, 2014).

5 REQUIRED INPUT DATA

5.1 InSAR processing

To generate the InSAR-based SD products, the required input data are:

- Sentinel-1 IW swath mode Single Look Complex images 2016–2023.
- 20 m NPI DEM (to remove the phase component related to topography, geocode and post-process the results) (NPI, 2014).
- DEM-based slope product (to discard sloping terrain > 5 degrees).
- Air temperature and precipitation from main meteorological stations (to compare with InSAR coherence and maximize the seasonal observation window) (NCCS, 2023).
- Glacier extents/outlines (to discard areas likely affected by phase jumps) (König et al., 2013; Lith et al., 2021).

Additional SAR data may be used (depending on availability in the study areas):

- TSX StripMap (2009–2017 in Adventdalen and Kapp Linné), PAZ StripMap (2023 in Adventdalen), RSAT-2 Fine-Mode (2009), ALOS-2 PALSAR (2022–2023 in Adventdalen) to test how variable radar frequencies and resolutions impact the results.

5.2 CryoGrid modelling

For the simulations, the input data are:

- ERA-5 reanalysis data (downscaled in the model framework).
- ESA CCI land cover for ground stratigraphy categorization.
- InSAR outputs as model inputs (SSD / MSD), including the coherence time series as uncertainty measure to weight the observations in the model.
- Potentially Sentinel-2 data to assess snow cover at pixel level.

For model validation, the following data will be used:

- Ground temperature from in-situ loggers in the permafrost monitoring sites of the study areas. The actual sites for these purposes are summarized in **Table 1**.
- Snow water equivalent / snow properties from manual measurements.
- Ground stratigraphy based on field investigations.

Table 1. Permafrost monitoring sites in the Option 7 study areas. Ground Temperature from boreholes (GT) and Active Layer Thickness from manual probing (ALT) will be used for validation (see also PVP).

Study area	Site name	Lat/long	Measured parameters	Available years	Monitoring network	Responsible institution	Comment and data access
ADV	ADV-B-1	78.189466, 16.149151	GT	2013–2023	GTN-P	UNIS	
ADV	ADV-B-2	78.194756, 15.985393	GT	2013–2023	GTN-P	UNIS	
ADV	AS-B-2	78.20146, 15.83465	GT	2008–2019	GNT-P	UNIS	

ADV	Adventdalen – Loess Terrace	78.2010, 15.8368	GT	2019–2023	SIOS	UNIS	Data access through MET
ADV	EN-B-1	78.190206, 15.78158	GT	2008–2021	GTN-P	UNIS	
ADV	EN-B-2	78.190456, 15.781619	GT	2013–2020	GTN-P	UNIS	
ADV	Endalen	78.1905, 15.7815	GT	2021–2023	SIOS	UNIS	Data access through MET
ADV	JAN-B-1	78.184726, 16.285834	GT	2013–2021	GTN-P	UNIS	
ADV	Innerhytte Pingo	78.1889, 16.3455	GT	2008–2020	GTN-P	UNIS	
ADV	Adventdalen – Innerhytta Pingo	78.1888, 16.3442	GT	2020–2023	SIOS	UNIS	Data access through MET
ADV	Ice Wedge	78.18583, 15.923572	GT	2012–2019	GTN-P	UNIS	
ADV	Adventdalen – Ice Wedge	78.18580, 15.92362	GT	2019–2023	SIOS	UNIS	Data access through MET
ADV	Snow-patch- lower	78.18752, 15.91324	GT	2008–2013	GTN-P	UNIS	
ADV	Snow-patch- upper	78.18752, 15.91324	GT	2008–2020	GTN-P	UNIS	
ADV	Adventdalen Upper Snowdrift	78.18752, 15.91328	GT	2019–2023	SIOS	UNIS	Data access through MET
ADV	Janssonhaugen – Vest	78.1794, 16.3686	GT	2019–2023	SIOS	MET	Data access through MET
ADV	Janssonhaugen	78.1793, 16.3805	GT	1998–2023	PACE	MET	Data access through MET
ADV	UNIS-CALM	78.2005, 15.8386	ALT	2000–2023	CALM	UNIS	
NYA	Bayelva	78.92086, 11.83345	GT	2009–2023	GNT-P	AWI	Data access through PANGEA
NYA	DBNyAlesund	78.92194, 11.86583	GT	2016–2019	GNT-P	UNIS	
NYA	Ecogrid	78.92, 11.86	ALT	2014–2019	CALM	University of Insubria	
KAP	KL-B-1	78.05663, 13.641478	GT	2008–2021	GNT-P	UNIS	
KAP	KL-B-2	13.636671, 78.054605	GT	2008–2021	GNT-P	UNIS	

6 OUTPUT PRODUCTS

The *IceInSAR* Option 7 output products are described in the PSD [RD-2] and summarized in **Table 2** and **Table 3** thereafter.

Table 2. Product specifications for the InSAR-based surface displacements (SD).

SD products	Unit	Property	Values provided	Product string
Seasonal SD time series	mm	SBAS-based displacement time series (2017–2021)	Displacement progression relative to first seasonal acquisition, maximal displacement during the season, coherence time series	SSD
Multi-seasonal SD maps	mm	Averaged maximal displacement of the seasons (2017–2021)	Mean, median and standard deviation of the maximal seasonal displacement (2017–2021), averaged coherence	MSD

Table 3. Product specification for the modelled ground temperature at a certain depth (GTD) and active layer thickness (ALT).

ECV variable	Unit	Property	Values provided	Product string
Ground temperature at certain depth (maximum 5 m)	degree C	At the local scale: daily modelled temperature At the regional scale: annual average	Results before and after InSAR-based SD assimilation.	GTD
Active layer thickness	m	At the local scale: daily thaw depth At the regional scale: annual maximum thaw depth	At the regional scale: Median and standard deviation of the ensemble	ALT

The Coordinate Reference System (CRS) used for the *IceInSAR* Option 7 in Svalbard will be projected in Transverse Mercator UTM 33N based on the World Geodetic System 1984 (WGS 1984) reference ellipsoid. The coordinates are specified in meters. Information on product projection, ellipsoid and pixel size will be included in the NetCDF.

7 PRACTICAL CONSIDERATIONS FOR IMPLEMENTATION

Due to the pilot nature of the project, the effect of InSAR SD assimilation on the performance of CryoGrid outputs will mostly be performed at specific locations where in-situ data is available for validation. For the **one-dimensional point-scale simulations**, no major issue is foreseen in term of implementation. The processing will be performed with well-established software (NORCE GSAR for the InSAR component and UiO CryoGrid for the modelling part). The procedure is meant to remain simple to first confirm/infirm the hypothesis that InSAR can contribute to improve the performance of the model. One challenge is related to the error quantification for InSAR products that is not well constrained especially in permafrost regions where in-situ surface displacement measurements are often lacking. We are exploring methodologies to the interferometric coherence time series used to weight the observation quality in the model (see Option 7 E3UB). The methodology for uncertainty documentation may evolve throughout the project.

The main unknowns are related to the **experimental products at the regional scale**. We will test the use of SSD and MSD products as model inputs to evaluate how they contribute to improve the model performance by constraining the parametrization of the ground stratigraphy based on the subsidence patterns during the thawing seasons and the spatial distribution of the movement amplitude within the selected regions. However, with the long-term objective to upscale the processing to larger areas, strategies to simplify the InSAR-based information and reduce the size of the input datasets are needed. A natural continuation of the project is therefore to test the generation and assimilation of a simplified InSAR-based geocryological map generated with clustering techniques. The idea is to provide SSD/MSD subproducts with few categories of ground movement amplitude/patterns that effectively represent various ground conditions while avoiding injecting unnecessary complexity having minor impact on the modelling results. Different clustering methods may be explored and the strategy to provide such simplified maps may therefore evolve throughout the project (see Option 7 ADP).

8 REFERENCES

8.1 Bibliography

- Aalstad, K., Westermann, S., Schuler, T. V., Boike, J., & Bertino, L. (2018). Ensemble-based assimilation of fractional snow-covered area satellite retrievals to estimate the snow distribution at Arctic sites. *The Cryosphere*, 12(1), 247–270.
- Aga, J., Boike, J., Langer, M., Ingeman-Nielsen, T., & Westermann, S. (2023). Simulating ice segregation and thaw consolidation in permafrost environments with the CryoGrid community model. *EGUsphere [preprint]*.
- Bamler, R., & Hartl, P. (1998). Synthetic aperture radar interferometry. *Inverse problems*, 14(4), R1.
- Baran, I., Stewart, M. P., Kampes, B. M., Perski, Z., & Lilly, P. (2003). A modification to the Goldstein radar interferogram filter. *IEEE Transactions on Geoscience and Remote Sensing*, 41(9), 2114–2118.
- Bartsch, A., Leibman, M., Strozzi, T., Khomutov, A., Widhalm, B., Babkina, E., ... & Bergstedt, H. (2019). Seasonal progression of ground displacement identified with satellite radar interferometry and the impact of unusually warm conditions on permafrost at the Yamal Peninsula in 2016. *Remote Sensing*, 11(16), 1865.
- Bartsch, A., Strozzi, T., & Nitze, I. (2023). Permafrost Monitoring from Space. *Surveys in Geophysics*, 1–35.
- Berardino, P., Fornaro, G., Lanari, R., & Sansosti, E. (2002). A new algorithm for surface deformation monitoring based on small baseline differential SAR interferograms. *IEEE Transactions on geoscience and remote sensing*, 40(11), 2375–2383.
- Chen, C. W., & Zebker, H. A. (2002). Phase unwrapping for large SAR interferograms: Statistical segmentation and generalized network models. *IEEE Transactions on Geoscience and Remote Sensing*, 40(8), 1709–1719.
- Fiddes, J., & Gruber, S. (2014). TopoSCALE v. 1.0: downscaling gridded climate data in complex terrain. *Geoscientific Model Development*, 7(1), 387–405.
- Goldstein, R. M., & Werner, C. L. (1998). Radar interferogram filtering for geophysical applications. *Geophysical Research Letters*, 25(21), 4035–4038.
- Hanssen, R. F. (2001). *Radar interferometry: data interpretation and error analysis* (Vol. 2). Springer Science & Business Media.
- König, M., Kohler, J., & Nuth, C. (2013). Glacier Area Outlines - Svalbard [Data set]. Norwegian Polar Institute. <https://doi.org/10.21334/npolar.2013.89f430f8>
- Larsen, Y., Engen, G., Lauknes, T. R., Malnes, E., & Høgda, K. A. (2006). A generic differential interferometric SAR processing system, with applications to land subsidence and snow-water equivalent retrieval. In Proceedings of Fringe 2005 Workshop, Frascati, Italy, 28 Nov.-2 Dec. 2005 (ESA SP-610, February 2006).
- Lauknes, T. R., Zebker, H. A., & Larsen, Y. (2010). InSAR deformation time series using an L_1 -norm small-baseline approach. *IEEE Transactions on Geoscience and Remote Sensing*, 49(1), 536–546.
- Lith, A., G. Moholdt & J. Kohler. (2021). Svalbard glacier inventory based on Sentinel-2 imagery from summer 2020 [Data set]. Norwegian Polar Institute. <https://data.npolar.no/dataset/1b8631bf-7710-449a-a56f-0da1a4fef608>
- Liu, L., Schaefer, K., Zhang, T., & Wahr, J. (2012). Estimating 1992–2000 average active layer thickness on the Alaskan North Slope from remotely sensed surface subsidence. *Journal of Geophysical Research: Earth Surface*, 117(F1).
- NCCS (2023). Seklima Observations and weather statics. Stations: Svalbard Airport (SN99840) and Adventdalen (99870). Ny-Ålesund (99910). Isfjord Radio (99790). <https://seklima.met.no/observations/>. Norwegian Centre for Climate Services.
- NPI (2014). Terrengmodell Svalbard (S0 Terrengmodell) [Data set]. Norwegian Polar Institute. <https://doi.org/10.21334/npolar.2014.dce53a47>.
- Obu, J., Westermann, S., Barboux, C., Bartsch, A., Delaloye, R., Grosse, G., Heim, B., Hugelius, G., Irrgang, A., Kääb, A.M., Kroisleitner, C., Matthes, H., Nitze, I., Pellet, C., Seifert, F.M., Strozzi, T., Wegmüller, U., Wiczorek, M., Wiesmann, A. (2021). ESA Permafrost Climate Change Initiative (Permafrost_cci): Permafrost Ground Temperature for the Northern

- Hemisphere, v3.0. NERC EDS Centre for Environmental Data Analysis, 28 June 2021. doi:10.5285/b25d4a6174de4ac78000d034f500a268. <https://dx.doi.org/10.5285/b25d4a6174de4ac78000d034f500a268>
- Obu, J., Westermann, S., Barboux, C., Bartsch, A., Delaloye, R., Grosse, G., Heim, B., Hugelius, G., Irrgang, A., Kääh, A.M., Kroisleitner, C., Matthes, H., Nitze, I., Pellet, C., Seifert, F.M., Strozzi, T., Wegmüller, U., Wiczorek, M., Wiesmann, A. (2021). ESA Permafrost Climate Change Initiative (Permafrost_cci): Permafrost active layer thickness for the Northern Hemisphere, v3.0. NERC EDS Centre for Environmental Data Analysis, 28 June 2021. <https://dx.doi.org/10.5285/67a3f8c8dc914ef99f7f08eb0d997e23>.
- Obu, J., Westermann, S., Barboux, C., Bartsch, A., Delaloye, R., Grosse, G., Heim, B., Hugelius, G., Irrgang, A., Kääh, A.M., Kroisleitner, C., Matthes, H., Nitze, I., Pellet, C., Seifert, F.M., Strozzi, T., Wegmüller, U., Wiczorek, M., Wiesmann, A. (2021). ESA Permafrost Climate Change Initiative (Permafrost_cci): Permafrost extent for the Northern Hemisphere, v3.0. NERC EDS Centre for Environmental Data Analysis, 28 June 2021. <https://dx.doi.org/10.5285/6e2091cb0c8b4106921b63cd5357c97c>
- Obu, J., Westermann, S., Bartsch, A., Berdnikov, N., Christiansen, H. H., Dashtseren, A., ... & Zou, D. (2019). Northern Hemisphere permafrost map based on TTOP modelling for 2000–2016 at 1 km² scale. *Earth-Science Reviews*, 193, 299–316.
- Reinosch, E., Buckel, J., Dong, J., Gerke, M., Baade, J., & Riedel, B. (2020). InSAR time series analysis of seasonal surface displacement dynamics on the Tibetan Plateau. *The Cryosphere*, 14(5), 1633–1650.
- Rouyet, L., Lauknes, T. R., Christiansen, H. H., Strand, S. M., & Larsen, Y. (2019). Seasonal dynamics of a permafrost landscape, Adventdalen, Svalbard, investigated by InSAR. *Remote Sensing of Environment*, 231, 111236.
- Rouyet, L., Liu, L., Strand, S. M., Christiansen, H. H., Lauknes, T. R., & Larsen, Y. (2021). Seasonal InSAR Displacements Documenting the Active Layer Freeze and Thaw Progression in Central-Western Spitsbergen, Svalbard. *Remote Sensing*, 13(15), 2977.
- Sandwell, D. T., & Price, E. J. (1998). Phase gradient approach to stacking interferograms. *Journal of Geophysical Research: Solid Earth*, 103(B12), 30183–30204.
- Schaefer, K., Liu, L., Parsekian, A., Jafarov, E., Chen, A., Zhang, T., ... & Schaefer, T. (2015). Remotely sensed active layer thickness (ReSALT) at Barrow, Alaska using interferometric synthetic aperture radar. *Remote sensing*, 7(4), 3735–3759.
- Strozzi, T., Antonova, S., Günther, F., Mätzler, E., Vieira, G., Wegmüller, U., ... & Bartsch, A. (2018). Sentinel-1 SAR interferometry for surface deformation monitoring in low-land permafrost areas. *Remote Sensing*, 10(9), 1360.
- Wang, C., Zhang, Z., Zhang, H., Wu, Q., Zhang, B., & Tang, Y. (2017). Seasonal deformation features on Qinghai-Tibet railway observed using time-series InSAR technique with high-resolution TerraSAR-X images. *Remote sensing letters*, 8(1), 1–10.
- Wang, C., Zhang, Z., Zhang, H., Zhang, B., Tang, Y., & Wu, Q. (2018). Active layer thickness retrieval of Qinghai-Tibet permafrost using the TerraSAR-X InSAR technique. *IEEE Journal of Selected Topics in Applied Earth Observations and Remote Sensing*, 11(11), 4403–4413.
- Wang, L., Marzahn, P., Bernier, M., & Ludwig, R. (2020). Sentinel-1 InSAR measurements of deformation over discontinuous permafrost terrain, Northern Quebec, Canada. *Remote Sensing of Environment*, 248, 111965.
- Westermann, S., Wollschläger, U., & Boike, J. (2010). Monitoring of active layer dynamics at a permafrost site on Svalbard using multi-channel ground-penetrating radar. *The Cryosphere*, 4(4), 475–487.
- Westermann, S., Langer, M., & Boike, J. (2011). Spatial and temporal variations of summer surface temperatures of high-arctic tundra on Svalbard—Implications for MODIS LST based permafrost monitoring. *Remote Sensing of Environment*, 115(3), 908–922.
- Westermann, S., Langer, M., Boike, J., Heikenfeld, M., Peter, M., Etzelmüller, B., & Krinner, G. (2016). Simulating the thermal regime and thaw processes of ice-rich permafrost ground with the land-surface model CryoGrid 3. *Geoscientific Model Development*, 9, 523–546.

- Westermann, S., Peter, M., Langer, M., Schwamborn, G., Schirrmeister, L., Etzelmüller, B., & Boike, J. (2017). Transient modeling of the ground thermal conditions using satellite data in the Lena River delta, Siberia. *The Cryosphere*, 11(3), 1441–1463.
- Westermann, S., Ingeman-Nielsen, T., Scheer, J., Aalstad, K., Aga, J., Chaudhary, N., ... & Langer, M. (2023). The CryoGrid community model (version 1.0) – a multi-physics toolbox for climate-driven simulations in the terrestrial cryosphere. *Geoscientific Model Development*. 16(9), 2607–2647.
- Zhang, X., Zhang, H., Wang, C., Tang, Y., Zhang, B., Wu, F., ... & Zhang, Z. (2019). Time-series InSAR monitoring of permafrost freeze-thaw seasonal displacement over Qinghai–Tibetan Plateau using Sentinel-1 data. *Remote Sensing*, 11(9), 1000.
- Zhang, X., Zhang, H., Wang, C., Tang, Y., Zhang, B., Wu, F., ... & Zhang, Z. (2020). Active layer thickness retrieval over the Qinghai-Tibet Plateau using Sentinel-1 multitemporal InSAR monitored Permafrost subsidence and temporal-spatial multilayer soil moisture data. *Ieee Access*, 8, 84336–84351.
- Zhao, R., Li, Z. W., Feng, G. C., Wang, Q. J., & Hu, J. (2016). Monitoring surface deformation over permafrost with an improved SBAS-InSAR algorithm: With emphasis on climatic factors modeling. *Remote Sensing of Environment*, 184, 276–287.
- Zwieback, S., & Meyer, F. J. (2021). Top-of-permafrost ground ice indicated by remotely sensed late-season subsidence. *The Cryosphere*, 15(4), 2041–2055.
- Zwieback, S., Liu, X., Antonova, S., Heim, B., Bartsch, A., Boike, J., & Hajnsek, I. (2016). A statistical test of phase closure to detect influences on DInSAR deformation estimates besides displacements and decorrelation noise: Two case studies in high-latitude regions. *IEEE Transactions on Geoscience and Remote Sensing*, 54(9), 5588–5601.

8.2 Acronyms

AD	Applicable Document
ADP	Algorithm Development Plan
ALT	Active Layer Thickness
ATBD	Algorithm Theoretical Basis Document
B.GEOS	b.geos GmbH
CCI	Climate Change Initiative
ECV	Essential Climate Variable
EO	Earth Observation
ESA	European Space Agency
E3UB	End-To-End ECV Uncertainty Budget
GAMMA	Gamma Remote Sensing AG
GCOS	Global Climate Observing System
GT	Ground Temperature
GTN-P	Global Terrestrial Network for Permafrost
UIO	University of Oslo
INSAR	Synthetic Aperature Radar Interferometry
IPA	International Permafrost Association
NORCE	Norwegian Research Centre AS
PE	Permafrost Extent
PF	Permafrost Fraction
PSD	Product Specification Document
PVASR	Product Validation and Algorithm Selection Report
PVP	Product Validation Plan

RD	Reference Document
RMSE	Root Mean Square Error
SAR	Synthetic Aperture Radar
SD	Surface Displacement
URD	Users Requirement Document
URq	User Requirement
WMO	World Meteorological Organisation